Free Radical Controlled Polymerization of Fluorinated Copolymers Produced in Microemulsion

Marco Apostolo,† Vincenzo Arcella,† Giuseppe Storti,‡ and Massimo Morbidelli*,‡

Swiss Federal Institute of Technology Zurich, Laboratorium für Technische Chemie/LTC, ETH Hönggerberg/HCI, CH-8093 Zurich, Switzerland, and Ausimont R&D, Via S.Pietro 50/A, I-20021 Bollate, Milano, Italy

Received November 13, 2001; Revised Manuscript Received April 24, 2002

ABSTRACT: Controlled free-radical polymerization is an emerging technique which can in principle produce macromolecules with well defined microstructure, possibly tailored to specific applications. This work describes the application of such a process to the production of several hundreds of tons of a fluorinated copolymer per year. The aim is to control the microstructure of the product and, in particular, to produce branched macromolecules with relatively uniform chain lengths. The process operates in microemulsion and is complicated by the presence of branching reactions. A complete kinetic model is developed to identify the most appropriate operating conditions to produce copolymers with desired characteristics.

1. Introduction

In a previous paper, we investigated the free-radical emulsion copolymerization of vinylidene fluoride (VDF) and hexafluoropropylene (HFP).[1] On the basis of the relatively small number of polymer samples accurately characterized in terms of molecular weight distribution, MWD, chain end groups, and branching degree, a reliable kinetic scheme for VDF−HFP copolymerization was formulated, and all of the involved kinetic parameters were estimated. According to the experimental results reported there, the copolymer produced without any chain transfer agent exhibited a significant degree of branching, with a polydispersity value around 5 and a calculated number of long branches per macromolecule around 1.4 at final conversion. These long branches are formed by chain transfer to polymer and propagation to terminal double bond (TDB). To reduce the degree of long chain branching in the system and, therefore, the broadness of the MWD, a chain transfer agent was used, thus obtaining a final polydispersity close to 3 and an average number of long branches per macromolecule around 0.4. However, the use of a chain transfer agent resulted in a significant reduction of the final average chain length, with a value around half of the one obtained without a chain transfer agent even when using a larger partial pressure of monomer to increase the probability of propagation. This work is focused on the experimental and modeling analysis of an alternative approach to obtain this MWD narrowing but without reducing the average molecular weight, based on the use of a controlled (or living) free-radical process. This is probably the first application of such a polymerization technique to an industrial process producing several hundreds of tons of polymer per year.

Free radical living polymerization provides a tool for controlling the microstructural properties of a polymer during its synthesis.[2] Through such a reaction mode, polymers and copolymers with well defined and homogeneous microstructure, i.e., narrow distributions of molecular weight, monomer sequences, chain ends, degree of branching, etc., are obtained. This process is readily feasible for anionic and cationic polymerizations of alkenes, ring-opening polymerizations, and various other ionic polymerizations.[3] In these cases, termination by combination is naturally prevented by the polarity of the chain ends, and transfer is the only irreversible chain-stopping event. More recently, free-radical living polymerizations were reported (cf. ref 2). Because in this case irreversible coupling terminations cannot be avoided, living conditions can only be approached by properly reducing termination, and therefore, these systems are sometimes referred to as pseudo-living polymerizations. Free-radical living polymerizations can also be used to build "tailor-made" block or graft copolymers.

Many different kinetic mechanisms that make living free-radical polymerization feasible are nowadays accessible and comprehensive reviews are available (cf. refs 2 and 4). Among these mechanisms, the so-called degenerative transfer is considered here, because it has been shown that it can be used in radical segregated systems while preserving large rates of polymerization.[5] In this case, a chain transfer agent is added to the system which does not affect the radical concentration, which is kept low by simply using very small amounts of initiator. The degenerative transfer reaction shifts the radical activity from chain to chain according to the following transfer reaction:

$$R_n + R_m X \xrightarrow{k_{ex}} R_n X + R_m \qquad (1)$$

where R_n indicates a radical of length n and $R_n X$ indicates the corresponding reversibly terminated chain. This continuous exchange of radical activity results in an intermittent growth of the polymer chains which lasts for the entire process and increases the chain length homogeneity. In this work, this mechanism is exploited to establish living conditions when copolymerizing the fluorinated monomers mentioned above using transfer agents containing iodine. These compounds have been indicated as effective by Oka and Tatemoto.[6] The energy of the carbon−iodine bond is low enough to transfer iodine from chain to chain according to reaction

* To whom correspondence should be addressed.
† Ausimont R&D.
‡ Swiss Federal Institute of Technology Zurich.

10.1021/ma0119575 CCC: $22.00
Published on Web 07/09/2002

1. In particular, di-iodine substituted fluorinated molecules with general formula $I-(CF_2)_n-I$ efficiently support living polymerization conditions. Moreover, to reduce irreversible bimolecular terminations as much as possible, a reduced amount of initiator, smaller than that typical of an ordinary free-radical emulsion polymerization by about 2 orders of magnitude, was used. The resulting low number of active chains per particle[7] leads to slow polymerization rates. Therefore, to obtain acceptable polymerization rates, the polymerization was performed in a microemulsion,[8] so as to compensate for the low reaction rate per particle by increasing the particle concentration. The microstructure of the resulting copolymer was characterized in terms of MWD, end groups, and degree of branching.

At the same time, we extended the kinetic model originally developed for the standard emulsion process[1] to living free-radical polymerization in microemulsion. The system is complicated by the presence of polymer branching reactions, which are typical of fluorinated polymers[9] and have to be accounted for in the model. This feature is unique with respect to all previous papers dealing with modeling of molecular weight distribution (MWD) and kinetic behavior of free-radical living homogeneous and heterogeneous polymerization, which only considered linear polymers.[10] The peculiarity of these systems is that a polymer chain can be reactivated not only by exchange but also by branching reactions. Therefore, no irreversible termination is present because even bimolecular termination or transfer to monomer do not prevent polymer chains from growing further. However, although degenerative exchange narrows the MWD, branching broadens the distribution. Thus, a mathematical model is needed to (i) identify the main features of such polymerization systems and (ii) analyze in a quantitative way the process response to variations of operating conditions and reaction recipe.

2. Experimental Section

2.1. Apparatus and Chemicals. The polymerization reactions were carried out in the pilot plant reactor described by Apostolo et al.[1] The reactor was a 10^{-2} m^3 volume, stainless steel vessel, equipped with two baffles and a stirrer with two three-bladed turbines. The stirring speed was always 550 rpm, a value sufficient to avoid monomer transport resistances from gas to liquid phase. During the reaction, a gaseous monomer mixture of suitable composition was continuously fed to the reactor in order to keep the pressure constant while producing a copolymer with constant composition.[11] Because the monomer accumulation in the three phases inside the reactor (gas, water, and particles) is negligible, the monomer feed flow rate is practically equal to the reaction rate, and the composition of the feed mixture is the same as that of the desired copolymer (VDF/HFP at molar ratio equal to 79/21). Therefore, because the instantaneous conversion is practically equal to 100% all along the process, the amount of produced copolymer has been used as evolutionary coordinate instead of conversion; that is, all experimental results are reported as a function of weight concentration of produced copolymer.

Vinylidene fluoride ($CH_2=CF_2$; purity 99.98%), hexafluoropropylene ($CF_3CF=CF_2$; purity 99.70%), and the iodine transfer agent ($C_6F_{12}I_2$; purity 98%) were used as produced by Ausimont. The free-radical initiator, $(NH_4)_2S_2O_8$ (Fluka; purity 98%), was used as received. The water was deionized and demineralized before usage.

The reaction was carried out in microemulsion.[8] Before starting the reaction, a thermodynamically stable dispersion of droplets, or micelles, of a fluorinated oil (Galden DO2 oil; purity 99%) and a fluorinated surfactant (Galden ammonium carboxylate, MW = 570 g/mol; purity 99%) in water is prepared with the composition detailed in Table 1. The initial diameter of these micelles was typically between 8 and 10 nm. Then, the reactor was charged with 6.5×10^{-5} m^3 of microemulsion and 6.5×10^{-3} m^3 of water. It was pressurized by charging the monomers and the polymerization was started by initiator addition. Under such diluted conditions, the resulting dispersion was no longer thermodynamically stable. However, the growth of droplet volume by coagulation and diffusion was much slower than the polymerization rate and can be neglected. Additional details on the microemulsion preparation and usage can be found in ref 8.

Table 1. Polymerization Recipe

pressure	2.2	MPa
temperature	353	K
water volume	6.5×10^{-3}	m^3
microemulsion		
volume	6.5×10^{-5}	m^3
water	58	%v
oil	15	%v
surfactant	27	%v
$(NH_4)_2S_2O_8$ concentration	0.05	kg m^{-3}
$C_6F_{12}I_2$ concentration	2.9	kg m^{-3}
gas feed composition		
HFP	21	mol %
VDF	79	mol %
particle number	7.3×10^{20}	m^{-3}
final polymer amount		
run 1	100	kg m^{-3}
run 2	200	kg m^{-3}
run 3	400	kg m^{-3}

2.2. Polymer Characterization. The MWD of the VDF/HFP copolymer was measured by gel permeation chromatography (GPC). The analyses were performed in tetrahydrofuran (Baker; RPE grade) at 30 °C using a constant flow rate of 1 cm^3/min supplied by a piston pump (Waters; model 590). Four Ultrastyragel styrene-divinylbenzene columns of porosity corresponding to 10^3, 10^4, 10^5, and 10^6 Å, respectively, were used. A detector based on refractive index measurement (HP 1047A) was adopted. In general, GPC with a single detector is inadequate to evaluate the MWD of branched polymers.[12] However, this procedure was effective for this specific copolymer,[13] mainly because of the limited long chain branching. In the referred paper, the procedure for MWD measurement is discussed and validated by the combined use of both fractioned and unfractioned samples. Moreover, the calibration was carried out using a series of copolymer standards of the same copolymer under examination (VDF/HFP, molar ratio 79/21), specifically synthesized.[14]

Type and average number of polymer chain end groups were measured by NMR. The measurements were performed using a Varian Unity 300 instrument, operating at 300 MHz. The polymer samples were dissolved in acetone-d6 (Aldrich; purity 99.6%). ^{1}H NMR spectra were used to determine the average number of chain ends per macromolecule. This was calculated by dividing the chain end concentration by the average number molecular weight (provided by GPC analysis). The overall average number of chain ends per macromolecule, diminished by two, provided the average number of branches per macromolecule.

The amount of iodine in the polymer was measured by wavelength-dispersive X-ray fluorescence spectrometry applied to polymer samples dissolved in methyl iso-butyl ketone (Carlo Erba; RPE grade).

The particle number was evaluated by light scattering using a Spectra Physics 2020 argon-ion laser operating at 514.5 nm with a BI2030AT correlator and a BI200SM goniometer (Brookhaven Instruments Co.). The reported values were measured at final conversion. Because the nucleation stage is very fast, this value is considered constant throughout the reaction when estimating the average number of active chains per particle.

initiation reaction

$I \xrightarrow{k_I} 2R_W$

bimolecular termination by entry

$R_W \xrightarrow{k_e} P_{n,i}$

propagation

$R_{n,i} + M \xrightarrow{K_p} R_{n+1,i}$ $\quad K_p = \sum_{i,l} k_{p,il}\phi_i f_l$

chain transfer to monomer

$R_{n,i} + M \xrightarrow{K_{fm}} P^{=}_{n,i} + R_{1,0}$ $\quad K_{fm} = \sum_{i,l} k_{fm,il}\phi_i f_l$

chain transfer to polymer

$R_{n,i} + P_{m,j} \xrightarrow{K_{fp}} P_{n,i} + R_{m,j}$ $\quad K_{fp} = \sum_{i,l} k_{p,il}\phi_i z_l$

propagation to TDB

$R_{n,i} + P^{=}_{m,j} \xrightarrow{K^*_p} R_{n+m,i+j}$ $\quad K^*_p = \sum_i k^*_{p,i}\phi_i$

degenerative transfer to di-iodine agent

$T_2 + R_{n,i} \xrightarrow{K_{ex1}} R_{1,1} + P_{n,i+1}$ $\quad K_{ex1} = \sum_i k_{ex1,i}\phi_i$

degenerative transfer to dormant chains

$R_{n,i} + P_{m,j} \xrightarrow{K_{ex}} R_{n,i-1} + P_{m,j+1}$ $\quad K_{ex} = \sum_i k_{ex,i}\phi_i$

desorption

$R_{1,0} \xrightarrow{k_d} R_W$

Figure 1. Kinetic scheme of VDF/HFP copolymerization along with the definition of the pseudo-kinetic rate constants, K_x. f_i = mole fraction of monomer i in the residual monomer mixture; ϕ_i = probability of a terminal unit of monomer i in the active polymer; z_i = mole fraction of monomer i in copolymer.

3. Kinetic Scheme

The kinetic scheme of VDF/HFP living copolymerization is shown in Figure 1, where I indicates the initiator in aqueous phase, M indicates the monomer in particle phase, T_2 indicates the di-iodine exchange agent in particle phase, R_W indicates the active oligomers in aqueous phase, and $R_{n,i}$ and $P_{n,i}$ indicate the radical and terminated chains containing n monomer units and i iodine chain ends in particle phase, respectively, whereas $P^{=}_{n,i}$ indicates a polymer chain with a terminal double bond in the particle phase. Note that $P_{n,0}$ corresponds to the terminated chains without iodine end atoms. This species, in contrast with $P_{n,i}$ for $i > 0$, cannot be reactivated by degenerative transfer. On the other hand, both types of terminated chains can be reactivated by chain transfer to polymer or propagation of the terminal double bond, if they happen to have one.

All reactions in Figure 1 have already been considered when modeling the standard (nonliving) emulsion process,[1] with the exception of degenerative transfer reactions, termination by radical entry into the particles, and radical desorption from the particles. Let us briefly comment on these additional kinetic terms.

In a previous work,[7] we studied the effect of radical entry and desorption for this same polymerization system, which is characterized by small amounts of initiator and small particle sizes, as we will see quantitatively in the following. Numerical values of the average number of active chains per particle in the range 0.11−0.40 were estimated under these conditions. As a consequence, this system can be classified as "Smith−Ewart Case I" (cf. ref 15), which implies radical loss by desorption and instantaneous termination by entry. This last termination is included in Figure 1 by merging the two consecutive events, entry and bimolecular termination, in a single step, the rate of which is equal to the entry rate. Note that this termination event actually involves a long chain radical and a very short radical just entered and, therefore, it would be regarded as a monomolecular termination with respect to the final MWD. On the other hand, under these conditions, the combination between two long chains is prevented, and therefore, the corresponding reaction is not included in Figure 1. The desorption rate constant, k_d, has been evaluated through the relation:

$$k_d = \frac{a}{r^2} \tag{2}$$

where r is the polymer particle radius and a is a parameter. Because monomers with very poor solubility in water are considered here, the following expression for a applies:

$$a = \frac{K_{fm}}{K_p}\frac{3\mathscr{D}_w}{m + 2\mathscr{D}_w/\mathscr{D}_p} \tag{3}$$

where m is the partition coefficient between particles and aqueous solution, and $\mathscr{D}_w$ and $\mathscr{D}_p$ are the diffusion coefficients of the monomeric radical in aqueous and particle phase, respectively. Equation 2 corresponds to the limiting case of complete reentry for the desorption law proposed by Asua et al.[16] Because the dependence of $\mathscr{D}_p$ on conversion can be ignored because in the particular case of constant pressure under examination the monomer-to-polymer ratio inside the particles remains constant, also a remains constant during the reaction.

About the transfer agent, fluorescence and NMR measurements performed on polymers produced at different conversions indicated that the amount of iodine found in the polymer chains is about 70% of the total iodine charged to the reactor. This is because under thermal initiation the decomposition of the iodofluorocarbon results in the production of some free iodine[17] and leaves an inert species no longer able to act as transfer agent. The rate constant of the reaction of abstraction of an iodine atom from the transfer agent, K_{ex1}, is different from that of iodine abstraction from a terminated polymer chain, K_{ex}. The iodine transfer agent is a low molecular weight species, and it is therefore more mobile than a polymer chain. Because the chemical bonds are very similar, K_{ex1} should be greater than K_{ex}.

The concentration of polymer chains with a TDB, $P^{=}_{n,i}$, is expressed as a fraction, $\alpha_{n,i}$, of the overall concentration of terminated chains, $P_{n,i}$. The developed model assumes that such a fraction is independent of chain length and number of iodine terminal units, which means $P^{=}_{n,i} = \alpha P_{n,i}$ with $\alpha < 1$. An implicit assumption underlying this approximation is that no chain contains more than one TDB. To account for the distribution of terminal double bonds, the approach recently proposed by Zhu and Hamielec[18] could be applied. However, in the system under examination, the presence of macrocross-linkers, i.e., macromolecules with two or more pendant double bonds, is negligible because of the relatively low degree of branching, as verified later experimentally.

Let us now consider the set of elementary reactions that constitute the overall kinetic scheme, together with the chain end groups that are left by each. As mentioned above, this set of reactions is equivalent to that considered in the earlier study[1] with the addition of the exchange reactions and termination by entry (besides the correction of misprints appearing in Figure 2 of ref

1 related to the backbiting reactions). The rate of chain transfer to polymer is proportional to chain length, because hydrogen abstraction can occur at any point of the terminated chain. Similarly, because degenerative transfer can occur through any of the *j* iodine ends of a terminated chain, $P_{m,j}$, its rate is proportional to *j*.

initiation reaction

$$SO_4^{\bullet -} + CH_2{=}CF_2 \xrightarrow{k_I} {}^{\bullet}CF_2CH_2OSO_3^- \xrightarrow{H_2O} {}^{\bullet}CF_2\mathbf{CH_2OH}$$

chain transfer to monomer

$$RCH_2CF_2^{\bullet} + CH_2{=}CF_2 \xrightarrow{k_{fm,11}} R\mathbf{CH{=}CF_2} + {}^{\bullet}CF_2\mathbf{CH_3}$$

chain transfer to polymer

$$RCH_2CF_2^{\bullet} + RCH_2R \xrightarrow{k_{fp,11}} RCH_2\mathbf{CF_2H} + RC^{\bullet}HR$$

propagation by addition to TDB

$$R^{\bullet} + R\mathbf{CH{=}CF_2} \xrightarrow{K_p^*} RC^{\bullet}HCF_2R$$

bimolecular termination by entry (disproportionation)

$$R_W \xrightarrow{k_e} R\mathbf{CH{=}CF_2}$$

degenerative transfer to di-iodine agent

$$C_6F_{12}I_2 + RCF_2^{\bullet} \xrightarrow{k_{ex1,1}} {}^{\bullet}CF_2C_4F_8\mathbf{CF_2I} + R\mathbf{CF_2I}$$

degenerative transfer to dormant chains

$$R_1\mathbf{CF_2I} + R_2CF_2^{\bullet} \xrightarrow{k_{ex,1}} R_1CF_2^{\bullet} + R_2\mathbf{CF_2I}$$

backbiting reactions

$$RCF_2CH_2CH_2CF_2CH_2CF_2^{\bullet} \xrightarrow{k_{bb,1}} RCF_2C^{\bullet}HCH_2CF_2CH_2\mathbf{CF_2H}$$

$$RCF_2CH_2CH_2CF_2CF_2CH_2^{\bullet} \xrightarrow{k_{bb,2}} RCF_2C^{\bullet}HCH_2CF_2CF_2\mathbf{CH_3}$$

The first type of chain end (CH_2OH) actually derives from the sulfate groups which fully react in the aqueous medium. The bimolecular termination by disproportionation after entry is assumed to produce a very low MW species originated by the collision between the short radical, R_W, and a long chain. Although the short chain is neglected with respect to the evaluation of the polymer microstructure, the long one is accounted for and its end group contains a TDB.

The backbiting reactions are considered only when calculating the chain ends but not when computing the polymerization kinetics; therefore, they are not included in Figure 1. The length of the formed branches is in fact so small to preclude their detection by the techniques typically used for long branches, such as GPC with multiple detectors (cf. ref 13). These backbiting reactions also do not affect the length of the chain and thus the MWD. Backbiting can occur only in active chains where the sequence of the last three monomer units is one of the two indicated in the last two reactions of the scheme above. The end of the growing chain must have a sequence of three VDF units where the third before the last, or the third before the last and the last, are inverted (head−head addition).

CF_2I chain end groups are produced by degenerative transfer to the di-iodine agent. Degenerative transfer to a dormant chain does not change the total number of CF_2I, because one is consumed and one is formed. However, when the degenerative exchange to a dormant chain involves an active chain with the last VDF unit inverted (head−head addition), the obtained chain end is CH_2I. This aspect will not be treated further in this work, and CF_2I indicates the sum of CF_2I and CH_2I. The only end group that can be "consumed" in the above scheme is the TDB.

4. Model Development

This section presents the model used to simulate the evolution of the living microemulsion copolymerization under examination. The material balances of the monomers, as well as monomer interphase partitioning equations, were reported by Apostolo et al.[1] This model uses the pseudo-kinetic approach,[19] so that the kinetic evolution of the system is described in terms of an equivalent homopolymer whose kinetic constants are suitable averages of the true copolymerization parameters. The main assumptions of the model are as follows: 1. negligible inter- and intraparticle mass transport limitations, 2. quasi-steady-state and long chain assumptions for the growing radicals, 3. average number of active chains per particle well below 0.5, 4. homogeneous particles, and 5. negligible water solubility of monomers.

The third assumption is actually the result of the analysis reported in ref 7, whereas the others have been discussed in ref 1. In the first work, a wide set of values of the average number of active chains per particle, $\bar{n}$, has been measured under largely different conditions in terms of initiator and particle concentration. By fitting these values using the Smith−Ewart equations, $\bar{n}$ was always well below 0.5 under operating conditions close to those considered in this work (i.e., small particle sizes and initiator concentrations). This behavior is in contrast to that of standard emulsion polymerization,[1] where the average number of radicals per particle is well above 10 and each particle behaves like a pseudo-bulk. In this case, the active chains are segregated in the polymer particles, and bimolecular terminations are restricted to pairs of short−long chains, as discussed above. This is represented in the kinetic scheme in Figure 1 by the additional termination by entry, whereas the classical bimolecular terminations are neglected.

4.1. Balance Equations and Monomer Partitioning. The mass balance equation for the generic *i*th monomer in a system of N_m monomer species in a semibatch reactor is given in ref 1:

$$\frac{dM_i^T}{dM_c} = Qw_i - \frac{K_{p,i}M_i}{\sum_j K_{p,j}M_j} = Qw_i - Y_i \qquad i = 1, ..., N_m \tag{4}$$

In the equations above, the independent variable is the molar concentration of consumed monomer, M_c, instead of time. Note that the mass of produced polymer per unit volume of water phase is given by M_cMW_c, where MW_c is the molecular weight of the average monomer

unit in the copolymer chain (82.1 g/mol). Because of the very limited compositional drift in the reaction under examination here (a variation of copolymer composition with conversion below 1% mol was measured), this last quantity is considered constant during the process. Furthermore, all concentrations are conventionally referred to the unit of volume of water phase, the only volume inside the reactor which remains constant during the entire reaction. M_i^T represents the overall molar concentration of the ith monomer in the reactor, Q represents the overall monomer feed flow rate specific to the amount of produced polymer (i.e., moles of monomer mixture fed per mole of consumed monomer mixture), w_i represents the monomer mole fraction in the feed, M_i represents the ith monomer concentration in the polymer particles, Y_i represents the copolymer instantaneous composition, and $K_{p,i}$ represents the average propagation rate constant. The latter, according to the pseudo-kinetic approach, is evaluated as follows:

$$K_{p,i} = \sum_{j=1}^{N_m} k_{p,ji}\phi_j \qquad i = 1, ..., N_m \tag{5}$$

being $k_{p,ji}$ the true propagation rate constants and ϕ_j the probability of having an active chain with terminal unit constituted by monomer j. The probability ϕ_j is in turn calculated as a function of the instantaneous composition of the monomer mixture in the polymer particles and the true cross-propagation rate constants, as described elsewhere.[19]

The molar concentration of the ith monomer in the gas phase, M_i^g, is calculated as follows:[1]

$$M_i^g = \frac{Py_iV_g}{zRTV_w}\mathrm{V} \tag{6}$$

where P represents the reactor pressure, y_i represents the monomer molar fraction in the gas phase, V_w and V_g represent the volumes of water and gas phase, respectively, z represents the compressibility factor, R represents the ideal gas constant, and T represents the reactor temperature. The value of z has been estimated using the Peng−Robinson equation of state.[20] The partitioning of the monomers between gas phase and polymer particles is described using a simple linear law:

$$M_i = h_iPy_i\frac{M_cMW_c}{\rho_c} \qquad i = 1, ..., N_m \tag{7}$$

where h_i represents the Henry constant of the ith monomer and ρ_c represents the polymer density.

We assume that the di-iodine transfer agent is insoluble in the aqueous phase and the initiator is insoluble in the organic phase. Both of these assumptions are justified by the chemical nature of the two compounds. The mass balance equations for both of these species are given below:

$$\frac{dT_2}{dM_c} = -\frac{K_{ex,1}T_2}{K_pM} \tag{8}$$

$$\frac{dI}{dM_c} = -\frac{k_II}{K_pMY_{0,0}}\frac{V_p}{V_w} \tag{9}$$

where T_2 and I indicate the transfer agent and initiator concentration per unit volume of water phase, k_I represents the initiator decomposition rate constant, and $K_{ex,1}$ and K_p represent the average exchange and propagation rate constants as defined in Figure 1, respectively.

4.2. Population Balance Equations. The population balance equations for active and terminated chains in polymer particles are obtained from the kinetic scheme shown in Figure 1. As mentioned above, we are assuming that desorbed radicals do not react in the water phase and completely reenter the particles. Accordingly, the overall rate of radical entry, $\mathscr{R}_e'$, can be expressed as follows:

$$\mathscr{R}_e' = k_eR_WN = \mathscr{R}_I' + \mathscr{R}_d' \tag{10}$$

where $\mathscr{R}_I'$ indicates the rate of production of new radicals by initiator decomposition ($= 2k_II\eta$) and $\mathscr{R}_d'$ the overall desorption rate ($= k_dY_{0,0}$). Note that this equation corresponds to the quasi-steady-state version of the material balance of the chains growing in aqueous phase. According to eq 10, the rate of radical entry is given by the sum of the two rates on the right-hand side, which are both independent of the concentration of the active species in the aqueous phase. Therefore, the actual concentration R_W does not need to be computed and the rate constant of radical entry, k_e, is no longer a model parameter.

Three different balances are considered, two for the newly born radicals with zero and one terminal iodine atoms, $R_{1,0}$ and $R_{1,1}$, respectively, and one for the generic radical with chain length larger than 1, i.e., $R_{n,i}$. This reflects the different initiation mechanisms of the polymer chains which can produce radicals either through initiator decomposition, thus bearing no terminal iodine atoms, or through abstraction of an iodine atom from the transfer agent, thus with a terminal iodine atom. Moreover, it is assumed that the only species diffusing between particles and water phase is $R_{1,0}$, thus neglecting desorption and reentry of monomeric radicals with an iodine end atom, $R_{1,1}$. This assumption appears to be very reasonable because, differently from the radicals produced by initiator decomposition, the radicals coming from the transfer agent have actually six carbon atoms and no polar end group and therefore are much less soluble in the aqueous phase.

The population balances are given by:

$$\frac{dR^{1,0}}{dM_c} = \frac{\mathscr{R}_eN_A}{N}\left(\frac{N}{N_A} - Y_{0,0}\right) - \frac{R_{1,0}}{Y_{0,0}} + C_{fm}\left(1 - \frac{R_{1,0}}{Y_{0,0}}\right) - R_{1,0}\frac{\mathscr{R}_eN_A}{N} + C_{fp}\left(\frac{P_{1,0}}{M} - \frac{Q_{1,0}}{M}\frac{R_{1,0}}{Y_{0,0}}\right) - C_p^*\alpha\frac{Q_{0,0}}{M}\frac{R_{1,0}}{Y_{0,0}} - 2C_{ex1}\frac{R_{1,0}}{Y_{0,0}}\frac{T_2}{M} + C_{ex}\left(\frac{P_{1,1}}{M} - \frac{R_{1,0}}{Y_{0,0}}\frac{Q_{0,1}}{M}\right) - \mathscr{R}_d \tag{11}$$

$$\frac{dR_{1,1}}{dM_c} = -\frac{R_{1,1}}{Y_{0,0}} - C_{fm}\frac{R_{1,1}}{Y_{0,0}} - R_{1,1}\frac{\mathscr{R}_eN_A}{N} + C_{fp}\left(\frac{P_{1,1}}{M} - \frac{Q_{1,0}}{M}\frac{R_{1,1}}{Y_{0,0}}\right) - C_p^*\alpha\frac{Q_{0,0}}{M}\frac{R_{1,1}}{Y_{0,0}} + 2C_{ex1}\frac{T_2}{M}\left(1 - \frac{R_{1,1}}{Y_{0,0}}\right) + C_{ex}\left(2\frac{P_{1,2}}{Y_{0,0}} - \frac{R_{1,1}}{Y_{0,0}}\frac{Q_{0,1}}{M}\right) \tag{12}$$

$$\frac{dR_{n,i}}{dM_c} = \frac{R_{n-1,i}}{Y_{0,0}} - \frac{R_{n,i}}{Y_{0,0}} - C_{fm}\frac{R_{n,i}}{Y_{0,0}} - R_{n,i}\frac{\mathcal{R}_e N_A}{N} + C_{fp}\left(n\frac{P_{n,i}}{M} - \frac{Q_{1,0}}{M}\frac{R_{n,i}}{Y_{0,0}}\right) - C_p^*\alpha\frac{Q_{0,0}}{M}\frac{R_{n,i}}{Y_{0,0}} + C_p^*\alpha\sum_{r=1}^{n-1}\sum_{j=0}^{i}\frac{R_{n-r,i-j}}{Y_{0,0}}\frac{P_{r,j}}{M} + C_{ex}(i+1)\frac{P_{n,i+1}}{M} - 2C_{ex1}\frac{R_{n,i}}{Y_{0,0}}\frac{T_2}{M} - C_{ex}\frac{R_{n,i}}{Y_{0,0}}\frac{Q_{0,1}}{M} \qquad n > 1,\ i \geq 0 \quad (13)$$

where N indicates the concentration of particles per unit volume of water phase, N_A indicates Avogadro's number, $\mathcal{R}_e$ indicates the entry rate specific to the molar amount of consumed monomer mixture, $\mathcal{R}_e' V_p/(K_p M Y_{0,0} V_w)$, and $\mathcal{R}_d$ indicates the specific desorption rate, $\mathcal{R}_d' V_p/(K_p M Y_{0,0} V_w)$. The parameters C_x (with x = fm, fp, ex1, ex, and p) are defined as ratios between the effective kinetic rate constant of the xth kinetic event, K_x, and the overall propagation rate constant, K_p. All of these parameters are defined in Figure 1. Finally, $Y_{m,j}$ and $Q_{m,j}$ represent the mth order moment with respect to chain length and the jth order moment with respect to iodine chain ends of the active and terminated chain distribution, respectively, and they are defined by:

$$Y_{m,j} = \sum_n n^m \sum_i i^j R_{n,i} \quad (14)$$

$$Q_{m,j} = \sum_n n^m \sum_i i^j P_{n,i} \quad (15)$$

where, as usual, all quantities are referred to the unit volume of water.

The population balance equations for the terminated chains are

$$\frac{dP_{n,0}}{dM_c} = C_{fm}\frac{R_{n,0}}{Y_{0,0}} + R_{n,0}\frac{\mathcal{R}_e N_A}{N} + C_{fp}\left(\frac{Q_{1,0}}{M}\frac{R_{n,0}}{Y_{0,0}} - n\frac{P_{n,0}}{M}\right) - C_p^*\alpha\frac{P_{n,0}}{M} \qquad n \geq 1 \quad (16)$$

$$\frac{dP_{n,i}}{dM_c} = C_{fm}\frac{R_{n,i}}{Y_{0,0}} + R_{n,i}\frac{\mathcal{R}_e N_A}{N} + C_{fp}\left(\frac{Q_{1,0}}{M}\frac{R_{n,i}}{Y_{0,0}} - n\frac{P_{n,i}}{M}\right) - C_p^*\alpha\frac{P_{n,i}}{M} + 2C_{ex1}\frac{R_{n,i-1}}{Y_{0,0}}\frac{T_2}{M} + C_{ex}\left(\frac{R_{n,i-1}}{Y_{0,0}}\frac{Q_{0,1}}{M} - i\frac{P_{n,i}}{M}\right) \qquad n \geq 1,\ i > 0 \quad (17)$$

These equations apply to the irreversibly terminated chains ($i = 0$) and to dormant chains ($i > 0$), respectively. The negative terms in the balance represent reactivation mechanisms, namely, transfer to polymer, terminal double bond propagation, and degenerative transfer. However, in addition to reactivate chains, transfer to polymer and terminal double bond propagation produce long chain branches.

The numerical solution of these infinite sets of ordinary differential equations has been carried out using the method of moments. The quasi-steady-state assumption (QSSA) has been introduced for all radical species. The final form of the model equations and the corresponding numerical solution are discussed in the Appendix. Note that the zero-order moment of the active chains of all types in the polymer particles, $Y_{0,0}$, is calculated as follows:

$$\frac{dY_{0,0}}{dM_c} = \frac{\mathcal{R}_e N_A}{N}\left(\frac{N}{N_A} - 2Y_{0,0}\right) - \mathcal{R}_d \quad (18)$$

This equation is no other than the classical Smith–Ewart equation for the number of particles with one active chain in a zero-one system.

4.3. Equations for Chain Ends and Short and Long Branches. In addition to the moments of the MWD, the model calculates the concentration of chain ends according to the kinetic scheme in Figure 1 through the following balances:

$$\frac{d(CH_2OH)}{dM_c} = \mathcal{R}_I\frac{V_p}{V_w} \quad (19)$$

$$\frac{d(CF_2H)}{dM_c} = C_{fp}\frac{Q_{1,0}}{M} + C_{bb}\beta\frac{1}{M}\frac{V_p}{V_w} \quad (20)$$

$$\frac{d(CH_3)}{dM_c} = C_{fm} + C_{bb}(1-\beta)\frac{1}{M}\frac{V_p}{V_w} \quad (21)$$

$$\frac{d(TDB)}{dM_c} = \frac{\mathcal{R}_e N_A}{N}Y_{0,0} + C_{fm} - C_p^*\alpha\frac{Q_{0,0}}{M} \quad (22)$$

$$\frac{d(CF_2I)}{dM_c} = 2C_{ex1}\frac{T_2}{M} \quad (23)$$

where $\mathcal{R}_I$ ($= \mathcal{R}_I'/(K_p M Y_{0,0})$) represents the initiation rate specific to the amount of produced polymer, α ($=$ TDB/$Q_{0,0}$) the average number of TDB per terminated chain and β ($= k_{bb}/(k_{bb1} + k_{bb2})$) the fraction of backbiting reactions which leads to CF_2H chain ends.

The evaluation of long and short chain branches, LCB and SCB, is performed through the following relations:

$$\frac{d(LCB)}{dM_c} = C_{fp}\frac{Q_{1,0}}{M} + C_p^*\alpha\frac{Q_{0,0}}{M} \quad (24)$$

$$\frac{d(SCB)}{dM_c} = C_{bb}\frac{1}{M}\frac{V_p}{V_w} \quad (25)$$

which reflect that LCBs are produced by chain transfer to polymer and propagation to TDB while SCBs by backbiting.

5. Experimental Validation of the Model

The model has been validated by comparison with the experimental results of a living copolymerization reaction of VDF and HFP carried out in microemulsion at the composition 79:21 mol %. Both monomers are gaseous at reaction conditions. Because of the difficulties found to develop a reliable sampling procedure during the reaction, three reactions with the same recipe have been repeated but stopped at different final conversions. The complete polymerization recipe is reported in Table 1.

5.1. Model Parameter Evaluation. The values of the model physicochemical parameters and of some rate constants used in the simulations are summarized in Table 2 along with the corresponding sources. These

Table 2. Values of the Physicochemical Model Parameters

parameter	numerical value			ref
k_I	9.0×10^{-5}		s^{-1}	25
η	0.18			1
$k_{p,11}/k_{p,12}$	5			9
$k_{p,22}/k_{p,21}$	0			9
ρ_c	1800		kg m^{-3}	26
	1	**2**		
h_i	3.1×10^{-7}	4.8×10^{-7}	kmol Pa^{1-} m^{-3}	26
critical temperature	303.0	358.6	K	26
critical pressure	4.37	3.20	MPa	26
acentric factor	0.17303	0.35796		26

Table 3. Numerical Values of the Model Kinetic Parameters

parameter	numerical value		ref
K_p	2.1×10^3	m^3 $kmol^{-1}$ s^{-1}	1
C_{fm}	6.5×10^{-4}		1
C_{fp}	2.8×10^{-5}		1
C_p^*	9.3×10^{-3}		1
C_{bb}	1.3×10^{-3}	kmol m^{-3}	1
β	0.85		1
k_d	$5.0 \times 10^{-17}/r^2$	s^{-1} (r is particle radius in m)	7
C_{ex1}	1		this work
C_{ex}	3.2×10^{-2}		this work

values have been in part taken from the literature and in part independently measured at the Ausimont laboratories. Note that the initiator efficiency value was slightly adjusted with respect to the original one (from 0.20 to 0.18), whereas the k_I value is different from the one we used in a previous paper (ref 1; $k_I = 17 \times 10^{-5}$ s^{-1}) because the pH under the reaction conditions typical of microemulsion is close to neutrality, whereas it is acid under standard emulsion conditions. The values of all the remaining kinetic parameters, as reported in Table 3, have been taken from our previous works on standard emulsion polymerization (refs 1 and 7) without any adjustment, except for the rate ratios of the exchange reactions, C_{ex1} and C_{ex}, which obviously appear only in this work and have been estimated by fitting the model predictions to the experimental data of MWD and polymerization rate.

The estimated value of C_{ex} is about 2 orders of magnitude smaller than C_{ex1}, thus reflecting the fact that it is easier to abstract iodine from the transfer agent than from a dormant polymer chain. As discussed in section 3, this difference should be ascribed to diffusion limitations of the polymer chain rather than to a difference in the intrinsic chemical reactivity of the two species. Moreover, because of the large reactivity of the transfer agent, comparable to that of the monomer, the value of C_{ex1} has been assumed equal to 1 (i.e., $K_{ex1} = K_p$). Larger values of C_{ex1} do not lead to any variation in the calculated results.

Only MWD and the polymerization rate have been used to fit the model adjustable parameters. Therefore, the agreement of the measured concentrations of the various chain end groups with the model predictions provides an independent validation of the reliability of the developed model.

5.2. Polymerization Rate and Active Chain Concentration. The experimental data of polymer mass concentration vs time are compared with the model predictions (continuous curve) in Figure 2. The shape of this curve is significantly affected by radical desorption. Because the larger the particle size, the smaller the radical loss by desorption, the predicted average

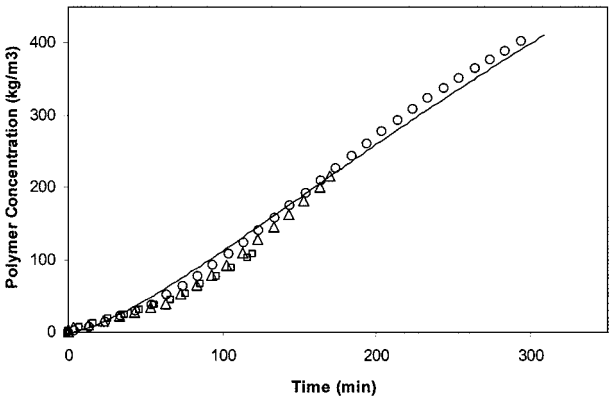

Figure 2. Polymer mass concentration as a function of time. Reaction recipe as in Table 1. Experimental data: □ = run 1; △ = run 2; ○ = run 3.

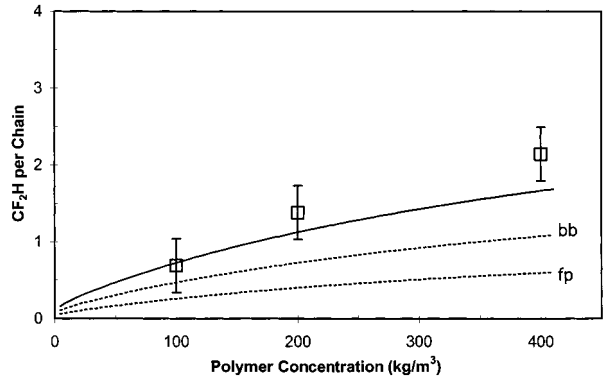

Figure 3. CF_2H end groups per chain as a function of polymer mass concentration. □ = experimental data. Continuous curve: model result. Dashed curves: contributions of backbiting (bb) and transfer to polymer (fp).

number of active chains per particle ranges from 0.05 at the beginning to about 0.15 at the end of the reaction. This increase of the average number of active chains explains the initial increase of polymerization rate observed experimentally. Moreover, in agreement with the experimental results, the calculated rate slightly decreases at the end of the polymerization reaction. This corresponds to the depletion of the initiator by thermal decomposition. To account for the loss of transfer agent through the mechanism described in section 3, an initial amount equal to 70% of the amount actually charged has been considered (cf. Table 1).

5.3. Chain Ends and Branching Distribution. The chain ends evolution as a function of conversion is shown in Figures 3 and 4 for CF_2H and CH_3, respectively. The good agreement between model predictions and experimental data confirms the observation that in this system terminations by disproportionation are quite limited, whereas they were instead one of the main sources of CF_2H chain end groups under standard emulsion conditions.[1] In Figure 3, the contributions to CF_2H formation by each of the two possible mechanisms in the kinetic scheme, i.e., backbiting (bb) and transfer to polymer (fp), are evidenced. The first one appears to be the most effective with this respect, in good agreement with the expected low degree of long chain branching in the final copolymer (cf. Figure 5). About the CH_3 end groups, they are almost completely formed by chain transfer to monomer, as it is evidenced by the dashed curves in Figure 4, which show the separate contributions of chain transfer to monomer (fm) and backbiting (bb).

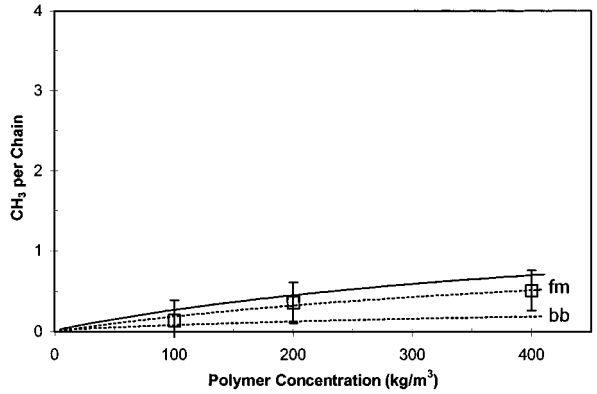

Figure 4. CH_3 end groups per chain as a function of polymer mass concentration. □ = experimental data. Continuous curve: model result. Dashed curves: contributions of backbiting (bb) and transfer to monomer (fm).

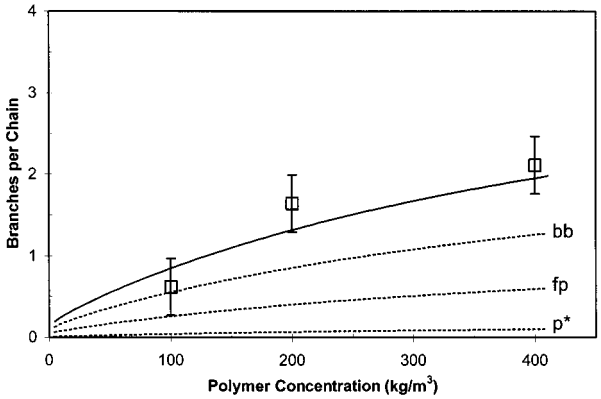

Figure 5. Branches per chain as a function of polymer mass concentration. □ = experimental data. Continuous curve: model result. Dashed curves: contributions of backbiting (bb), transfer to polymer (fp) and propagation to terminal double bond (p*).

The evolution of the number of branches per macromolecule as a function of conversion is shown in Figure 5. These experimental values were obtained by NMR and, therefore, represent the sum of long branches (formed by transfer to polymer, fp, and propagation to TDB, p*) and short branches (produced by backbiting, bb). Most branches are short, with long branches being about 0.5 per chain at the end of the reaction.

5.4. Iodine End Atoms Distribution. The CF_2I chain end groups predicted by the model are compared with the experimental results in Figure 6. These data can be interpreted by noting that, in the absence of transfer to the monomer, propagation to TDB, and termination by entry, the number of iodine end groups per chain can be easily calculated through the following equation:

$$CF_2I = \frac{2T_2^0}{T_2^0 + 2\eta I^0} \tag{26}$$

where T_2^0 and I^0 indicate the initial molar amounts of transfer agent and initiator, respectively. This relation follows from the fact that, after the complete depletion of the initial amount of iodine transfer agent, all iodine atoms are linked to polymer chains whose concentration is given by the sum of the concentration of the "effective" initiator fragments and of the initial iodine transfer agent. Because $T_2^0 \gg 2\eta I^0$, according to eq 26,

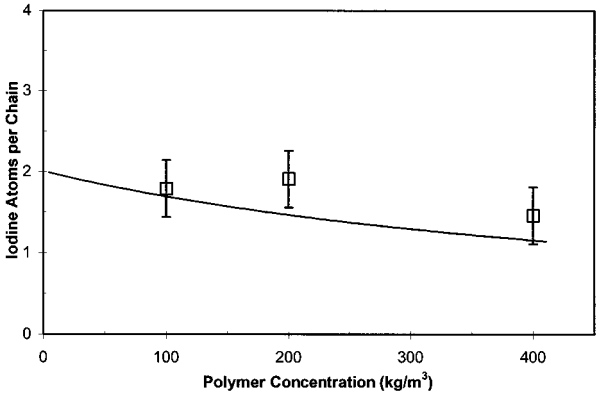

Figure 6. Iodine end atoms per chain as a function of polymer mass concentration. □ = experimental data. Continuous curve: model result.

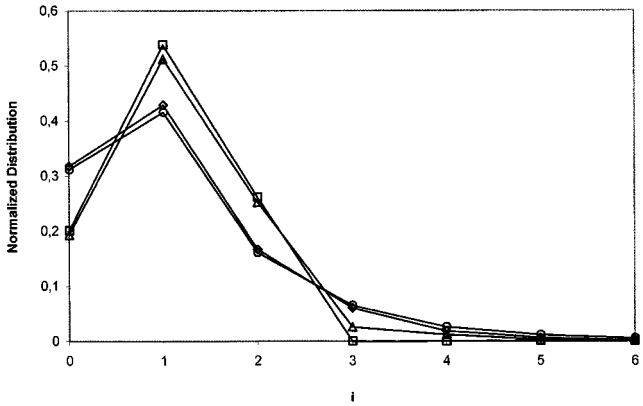

Figure 7. Calculated normalized distribution of iodine end atoms per chain at final conversion. ○ = all mechanisms accounted for; △ = without chain transfer to polymer; ◇ = without propagation to TDB; □ = without both chain transfer to polymer and propagation to TDB.

the number of CF_2I per chain should be very close to 2. However, chain transfer to the monomer and propagation to TDB are present in the system under examination, and they have to be accounted for. The first reaction reduces the number of iodine end groups per chain by producing a polymer chain with a TDB and a new active chain without an iodine terminal unit. In contrast, propagation to TDB decreases the number of chains, and then the number of CF_2I terminal units per chain increases. The combined effect of these reactions leads to the behavior shown in Figure 6. At the beginning of the polymerization, the number of iodine end groups per chain is close to 2. However, for increasing conversion values, transfer to the monomer prevails and produces the observed decrease down to about 1.2.

The calculated distribution of iodine end atoms per chain at final conversion is shown in Figure 7. The maximum number of iodine atoms per chain, *i*, is about 6. Because all model calculations have been performed with maximum number of iodine atoms per chain $NI = 15$ (cf. Appendix), the reconstruction of this distribution is sufficiently accurate. In the same figure, the distributions calculated without chain transfer to polymer ($C_{fp} = 0$), without propagation to TDB ($C_p^* = 0$) and without both these branching mechanisms ($C_{fp} = C_p^* = 0$) are shown for comparison. It can be seen that in the last case (no branching reactions), the distribution is limited to a maximum value of $i = 2$, because chains with larger numbers of chain ends cannot be formed.

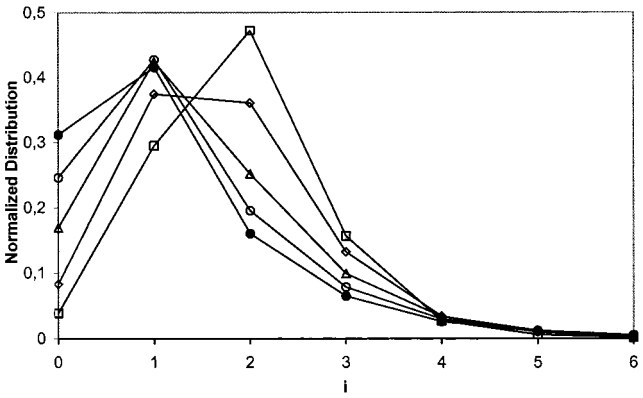

Figure 8. Calculated distribution of iodine end atoms per chain at various weight percentage conversions. □ = 1%; ◇ = 25%; △ = 50%; ○ = 75%; ● = 100%.

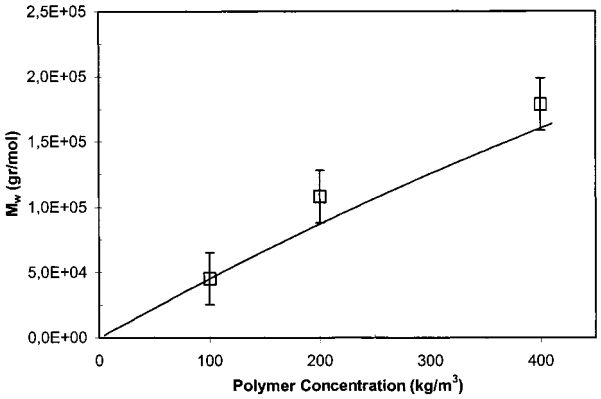

Figure 9. Weight average molecular weight, M_w, as a function of polymer mass concentration. □ = experimental data. Calculated results: continuous curve.

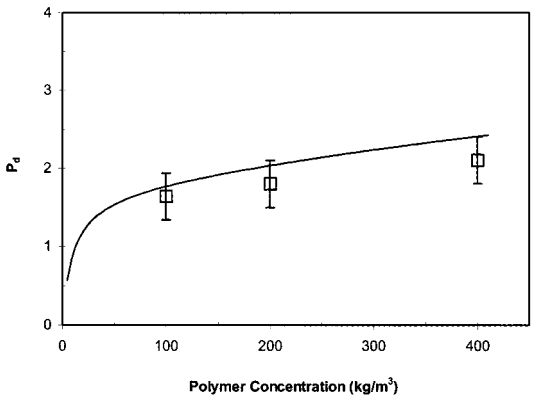

Figure 10. MWD polydispersity, P_d, as a function of polymer mass concentration. □ = experimental data. Continuous curve: model result.

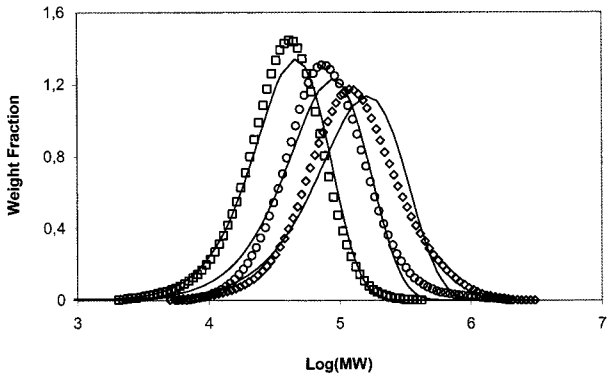

Figure 11. Copolymer MWD at increasing polymer mass concentrations. Experimental data: □ = 100 kg/m^3; ○ = 200 kg/m^3; ◇ = 400 kg/m^3. Continuous curves: model results.

On the other hand, both branching mechanisms lead to a broadening of this distribution, although to a rather different extent. In particular, it can be seen that the effect of propagation to TDB is much smaller, thus indicating that the dominating mechanism with respect to iodine group distribution is chain transfer to polymer.

The evolution of the same distribution as a function of conversion is shown in Figure 8. Following the discussion above, the frequency of macromolecules with two CF_2I end groups decreases with conversion; at the end of the reaction, most chains have one or no CF_2I end groups. In particular, the increase of polymer chains with no iodine chain end with conversion reflects the continuos increase of the number of chains initiated by chain transfer to monomer.

5.5. Molecular Weight Distribution. Figure 9 compares the experimental and calculated values of weight average molecular weight, M_w, as a function of conversion. The continuous increase of M_w is typical of living conditions.[2] A standard free radical polymerization carried out in a system controlled by chain transfer to monomer with no branching and constant monomer pressure (i.e., constant monomer concentration in particle) would in fact lead to a constant value of M_w all along the reaction. In this case, each chain during a single growth period adds a number of units that can be estimated as the ratio between the characteristic times of propagation and degenerative transfer to dormant chains, i.e., $M/2C_{ex}T_2$, where T_2 ($= T_2^0$) represents the total concentration of iodine groups per unit volume of water. This ratio varies during the polymerization because of the change of particle size and ranges from a very low value to a maximum of about 34 at the end of the reaction. This value, when compared to the overall chain length, is sufficiently low to guarantee a high homogeneity among all of the chains in the system, in agreement with the basic idea of living free-radical polymerization.

Figure 10 shows the polydispersity ratio, P_d, as a function of conversion. In contrast to the case of living polymerization of linear polymers,[2] after the initial increase, the curve does not exhibit a decrease but a slight increase with conversion. This behavior is the result of the counteracting effects of degenerative transfer, which produces a MWD narrowing, and transfer to polymer and propagation to TDB, which result in MWD broadening. In all cases, the resulting molecular weight distributions are much narrower than those obtained with nonliving free radical polymerization. As already mentioned, when producing this same copolymer in standard emulsion,[1] larger polydispersity values are obtained, i.e., 3 to 6 in Figure 5B of ref 1 against about 2 in Figure 10. The experimental and calculated molecular weight distributions corresponding to the average data shown in Figures 9 and 10 are compared in Figure 11. The peak of the molecular weight distribution moves toward high molecular weights as conversion increases, whereas the polydispersity index exhibits only a weak increase.

6. Concluding Remarks

The feasibility of the controlled copolymerization of fluorinated monomers (VDF and HFP) in microemulsion

has been established. The livingness of the process has been obtained by a degenerative transfer reaction with a transfer agent containing iodine atoms which are frequently transferred from chain to chain. The living polymerizations have been performed in microemulsion in order to obtain sufficiently large polymerization rates. This living process requires in fact such a small amount of initiator that, in standard emulsion polymerization conditions, these would be exceedingly slow. The resulting polymerization rate was only about 4 times slower than the standard emulsion process, thus exhibiting a satisfactory productivity from the industrial viewpoint.

About the microstructure of the polymer, a significant reduction of polydispersity was found, with a final value around 2.3, which is a remarkably small value for a system where various branching mechanisms are present. This MWD narrowing is superior to that obtained when using a chain transfer agent,[1] thus indicating the effectiveness of the living process. The efficiency of the trapping by the iodine atoms diminishes somewhat during the process, just because of the branching reactions. However, the living nature of the reaction does not seem to be affected, as proved by the reasonable linearity of the average molecular weight with conversion.

These experimental results agreed well with those calculated using a model with most of the parameter values given a priori as estimated in previous works (refs 1 and 7) and two adjustable parameters only, the exchange rate constants.

Finally, on the basis of the living microemulsion polymerization process presented here, Ausimont has developed a new polymerization technology called "branching & living".[24] This technology, successfully scaled to the industrial production, is currently used to produce hundreds of tons per year of special fluoroelastomer grades.

7. Appendix

The moment equations for the population balances are obtained through the moment generating function method.[21] It should be noted that the distribution is bivariate because two internal coordinates, i.e., the number of monomer units, n, and the number of iodine atoms, i, are considered. However, as the number of iodine atoms per chain, NI, is low (usually less than 15), the method of moments is applied only to monomer units, whereas each distribution with a different number of iodine units is considered individually. In other words, we write the MWD moment equations for polymer chains with $i = 0, 1, ..., NI$.

From eqs 11−13, the following expressions are obtained for 0th order moments of the active chain distribution as a function of polymer conversion:

$$\frac{dy_{0,0}}{dM_c} = \frac{\mathscr{R}_e N_A}{N}\left(\frac{N}{N_A} - Y_{0,0}\right) + C_{fm}\left(1 - \frac{y_{0,0}}{Y_{0,0}}\right) - y_{0,0}\frac{\mathscr{R}_e N_A}{N} + C_{fp}\left(\frac{q_{1,0}}{M} - \frac{Q_{1,0}}{M}\frac{y_{0,0}}{Y_{0,0}}\right) - \mathscr{R}_d - C_p^*\alpha\frac{Q_{0,0} - q_{0,0}}{M}\frac{y_{0,0}}{Y_{0,0}} - 2C_{ex1}\frac{y_{0,0}}{Y_{0,0}}\frac{T_2}{M} + C_{ex}\left(\frac{q_{0,1}}{M} - \frac{y_{0,0}}{Y_{0,0}}\frac{Q_{0,1}}{M}\right) \quad (27)$$

$$\frac{dy_{0,1}}{dM_c} = -C_{fm}\frac{y_{0,1}}{Y_{0,0}} + C_{fp}\left(\frac{q_{1,1}}{M} - \frac{Q_{1,0}}{M}\frac{y_{0,1}}{Y_{0,0}}\right) - y_{0,1}\frac{\mathscr{R}_e N_A}{N} - C_p^*\alpha\left[\frac{y_{0,1}}{Y_{0,0}}\left(\frac{q_{0,0}}{M} - \frac{Q_{0,0}}{M}\right) + \frac{y_{0,0}}{Y_{0,0}}\frac{q_{0,1}}{M}\right] - 2C_{ex1}\frac{T_2}{M}\left(1 - \frac{y_{0,1}}{Y_{0,0}}\right) + C_{ex}\left(2\frac{q_{0,2}}{M} - \frac{y_{0,1}}{Y_{0,0}}\frac{Q_{0,1}}{M}\right) \quad (28)$$

$$\frac{dy_{0,i}}{dM_c} = -C_{fm}\frac{y_{0,i}}{Y_{0,0}} + C_{fp}\left(\frac{q_{1,i}}{M} - \frac{Q_{1,0}}{M}\frac{y_{0,i}}{Y_{0,0}}\right) - y_{0,i}\frac{\mathscr{R}_e N_A}{N} + C_p^*\alpha\left(\sum_{j=0}^{i}\frac{y_{0,i-j}}{Y_{0,0}}\frac{q_{0,j}}{M} - \frac{Q_{0,0}}{M}\frac{y_{0,i}}{Y_{0,0}}\right) - 2C_{ex1}\frac{y_{0,i}}{Y_{0,0}}\frac{T_2}{M} + C_{ex}\left[(i+1)\frac{q_{0,i+1}}{M} - \frac{y_{0,i}}{Y_{0,0}}\frac{Q_{0,1}}{M}\right] \quad (i \geq 2) \quad (29)$$

where $y_{0,i}$ and $q_{0,i}$ indicate the 0th order moment of the distribution of active chains and dormant chains with i iodine atoms, respectively.

Similarly, the first-order moment equations of active chain distribution, $y_{0,i}$, are given by:

$$\frac{dy_{1,0}}{dM_c} = \frac{\mathscr{R}_e N_A}{N}\left(\frac{N}{N_A} - Y_{0,0}\right) + \frac{y_{0,0}}{Y_{0,0}} + C_{fm}\left(1 - \frac{y_{1,0}}{Y_{0,0}}\right) - \mathscr{R}_d + C_{fp}\left(\frac{q_{2,0}}{M} - \frac{Q_{1,0}}{M}\frac{y_{1,0}}{Y_{0,0}}\right) + C_p^*\alpha\left[\frac{q_{1,0}}{M}\frac{y_{0,0}}{Y_{0,0}} + \frac{y_{1,0}}{Y_{0,0}}\left(\frac{q_{0,0}}{M} - \frac{Q_{0,0}}{M}\right)\right] - 2C_{ex1}\frac{y_{1,0}}{Y_{0,0}}\frac{T_2}{M} + C_{ex}\left(\frac{q_{1,1}}{M} - \frac{y_{1,0}}{Y_{0,0}}\frac{Q_{0,1}}{M}\right) - y_{1,0}\frac{\mathscr{R}_e N_A}{N} \quad (30)$$

$$\frac{dy_{1,1}}{dM_c} = \frac{y_{0,1}}{Y_{0,0}} - C_{fm}\frac{y_{1,1}}{Y_{0,0}} + C_{fp}\left(\frac{q_{2,1}}{M} - \frac{Q_{1,0}}{M}\frac{y_{1,1}}{Y_{0,0}}\right) + C_p^*\alpha\left[\frac{y_{1,1}}{Y_{0,0}}\left(\frac{q_{0,0}}{M} - \frac{Q_{0,0}}{M}\right) + \frac{y_{0,1}}{Y_{0,0}}\frac{q_{1,0}}{M} + \frac{y_{0,0}}{Y_{0,0}}\frac{q_{1,1}}{M} + \frac{y_{1,0}}{Y_{0,0}}\frac{q_{0,1}}{M}\right] + 2C_{ex1}\frac{T_2}{M}\left(1 - \frac{y_{1,1}}{Y_{0,0}}\right) + C_{ex}\left(2\frac{q_{1,2}}{M} - \frac{y_{1,1}}{Y_{0,0}}\frac{Q_{0,1}}{M}\right) - y_{1,1}\frac{\mathscr{R}_e N_A}{N} \quad (31)$$

$$\frac{dy_{1,i}}{dM_c} = \frac{y_{0,i}}{Y_{0,0}} - C_{fm}\frac{y_{1,i}}{Y_{0,0}} + C_{fp}\left(\frac{q_{2,i}}{M} - \frac{Q_{1,0}}{M}\frac{y_{1,i}}{Y_{0,0}}\right) + C_p^*\alpha\left[\sum_{j=0}^{i}\left(\frac{y_{1,i-j}}{Y_{0,0}}\frac{q_{0,j}}{M} + \frac{y_{0,i-j}}{Y_{0,0}}\frac{q_{1,j}}{M}\right) - \frac{Q_{0,0}}{M}\frac{y_{1,i}}{Y_{0,0}}\right] - 2C_{ex1}\frac{y_{1,i}}{Y_{0,0}}\frac{T_2}{M} + C_{ex}\left[(i+1)\frac{q_{1,i+1}}{M} - \frac{y_{1,i}}{Y_{0,0}}\frac{Q_{0,1}}{M}\right] - y_{1,i}\frac{\mathscr{R}_e N_A}{N} \quad (i \geq 2) \quad (32)$$

whereas the second-order moments are given as follows:

$$\frac{dy_{2,0}}{dM_c} = \frac{\mathscr{R}_e N_A}{N}\left(\frac{N}{N_A} - Y_{0,0}\right) + \frac{y_{0,0}}{Y_{0,0}} + 2\frac{y_{1,0}}{Y_{0,0}} + C_{fm}\left(1 - \frac{y_{2,0}}{Y_{0,0}}\right) + C_{fp}\left(\frac{q_{3,0}}{M} - \frac{Q_{1,0}}{M}\frac{y_{2,0}}{Y_{0,0}}\right) + C_p^*\alpha\left[\frac{q_{2,0}}{M}\frac{y_{0,0}}{Y_{0,0}} + 2\frac{q_{1,0}}{M}\frac{y_{1,0}}{Y_{0,0}} + \frac{y_{2,0}}{Y_{0,0}}\left(\frac{q_{0,0}}{M} - \frac{Q_{0,0}}{M}\right)\right] - 2C_{ex1}\frac{y_{2,0}}{Y_{0,0}}\frac{T_2}{M} + C_{ex}\left(\frac{q_{2,1}}{M} - \frac{y_{2,0}}{Y_{0,0}}\frac{Q_{0,1}}{M}\right) - \mathscr{R}_d - y_{2,0}\frac{\mathscr{R}_e N_A}{N} \quad (33)$$

$$\frac{dy_{2,1}}{dM_c} = \frac{y_{0,1}}{Y_{0,0}} + 2\frac{y_{1,1}}{Y_{0,0}} - C_{fm}\frac{y_{2,1}}{Y_{0,0}} + C_{fp}\left(\frac{q_{3,1}}{M} - \frac{Q_{1,0}}{M}\frac{y_{2,1}}{Y_{0,0}}\right) + C_p^*\alpha\left[\frac{y_{2,1}}{Y_{0,0}}\left(\frac{q_{0,0}}{M} - \frac{Q_{0,0}}{M}\right)\right] + C_p^*\alpha\left(\frac{y_{2,0}}{Y_{0,0}}\frac{q_{0,1}}{M} + 2\frac{y_{1,0}}{Y_{0,0}}\frac{q_{1,1}}{M} + \frac{y_{0,0}}{Y_{0,0}}\frac{q_{2,1}}{M} + 2\frac{y_{1,1}}{Y_{0,0}}\frac{q_{1,0}}{M} + \frac{y_{0,1}}{Y_{0,0}}\frac{q_{2,0}}{M}\right) + 2C_{ex1}\frac{T_2}{M}\left(1 - \frac{y_{2,1}}{Y_{0,0}}\right) + C_{ex}\left(2\frac{q_{2,2}}{M} - \frac{y_{2,1}}{Y_{0,0}}\frac{Q_{0,1}}{M}\right) - y_{2,1}\frac{\mathscr{R}_e N_A}{N} \quad (34)$$

$$\frac{dy_{2,i}}{dM_c} = \frac{y_{0,i}}{Y_{0,0}} + 2\frac{y_{1,i}}{Y_{0,0}} - C_{fm}\frac{y_{2,i}}{Y_{0,0}} + C_{fp}\left(\frac{q_{3,i}}{M} - \frac{Q_{1,0}}{M}\frac{y_{2,i}}{Y_{0,0}}\right) + C_p^*\alpha\left[\sum_{j=0}^{i}\left(\frac{y_{2,i-j}}{Y_{0,0}}\frac{q_{0,j}}{M} + 2\frac{y_{1,i-j}}{Y_{0,0}}\frac{q_{1,j}}{M} + \frac{y_{0,i-j}}{Y_{0,0}}\frac{q_{2,j}}{M}\right) - \frac{Q_{0,0}}{M}\frac{y_{2,i}}{Y_{0,0}}\right] - 2C_{ex1}\frac{y_{2,i}}{Y_{0,0}}\frac{T_2}{M} + C_{ex}\left[(i+1)\frac{q_{2,i+1}}{M} - \frac{y_{2,i}}{Y_{0,0}}\frac{Q_{0,1}}{M}\right] - y_{2,i}\frac{\mathscr{R}_e N_A}{N} \quad (i \geq 2) \quad (35)$$

When the QSSA is applied, the system of differential equations 27−35 reduces to a system of algebraic equations.

In the case of terminated polymer chains, the following set of equations is readily obtained from eqs 16 and 17:

$$\frac{dq_{0,i}}{dM_c} = C_{fm}\frac{y_{0,i}}{Y_{0,0}} - C_{fp}\left(\frac{q_{1,i}}{M} - \frac{Q_{1,0}}{M}\frac{y_{0,i}}{Y_{0,0}}\right) - C_p^*\alpha\frac{q_{0,i}}{M} + y_{0,i}\frac{\mathscr{R}_e N_A}{N} + 2C_{ex1}\delta_i\frac{y_{0,i-1}}{Y_{0,0}}\frac{T_2}{M} + C_{ex}\left(-i\frac{q_{0,i}}{M} + \delta_i\frac{y_{0,i-1}}{Y_{0,0}}\frac{Q_{0,1}}{M}\right) \quad (i \geq 0) \quad (36)$$

$$\frac{dq_{1,i}}{dM_c} = C_{fm}\frac{y_{1,i}}{Y_{0,0}} - C_{fp}\left(\frac{q_{2,i}}{M} - \frac{Q_{1,0}}{M}\frac{y_{1,i}}{Y_{0,0}}\right) - C_p^*\alpha\frac{q_{1,i}}{M} + y_{1,i}\frac{\mathscr{R}_e N_A}{N} + 2C_{ex1}\delta_i\frac{y_{1,i-1}}{Y_{0,0}}\frac{T_2}{M} + C_{ex}\left(-i\frac{q_{1,i}}{M} + \delta_i\frac{y_{1,i-1}}{Y_{0,0}}\frac{Q_{0,1}}{M}\right) \quad (i \geq 0) \quad (37)$$

$$\frac{dq_{2,i}}{dM_c} = C_{fm}\frac{y_{2,i}}{Y_{0,0}} - C_{fp}\left(\frac{q_{3,i}}{M} - \frac{Q_{1,0}}{M}\frac{y_{2,i}}{Y_{0,0}}\right) - C_p^*\alpha\frac{q_{2,i}}{M} + 2C_{ex1}\delta_i\frac{y_{2,i-1}}{Y_{0,0}}\frac{T_2}{M} + C_{ex}\left(-i\frac{q_{2,i}}{M} + \delta_i\frac{y_{2,i-1}}{Y_{0,0}}\frac{Q_{0,1}}{M}\right) + y_{2,i}\frac{\mathscr{R}_e N_A}{N} \quad (i \geq 0) \quad (38)$$

where $\delta_i = 1$ for $i > 0$ and $\delta_i = 0$ for $i = 0$.

In the equations above, the third-order moments with respect to the chain length $q_{3,i}$ are needed. They have been evaluated through the following closure formula, based on the approximation of the unknown distribution as a truncated series of Laguerre polynomials using a gamma distribution weighing function:[22]

$$q_{3,0} = 2\frac{{q_{2,0}}^2}{q_{1,0}} - \frac{q_{2,0}}{q_{0,0}}q_{1,0} \quad (39)$$

This formula has been proved effective for the case of nonlinear chains by Baltsas et al.[23]

From the moments of the MWDs of each type of polymer chains (i.e., with different number of iodine units), the overall moments $Y_{m,j}$ and $Q_{m,j}$ are evaluated as follows:

$$Y_{m,j} = \sum_{k=0}^{\infty} k^j y_{m,k};\ Q_{m,j} = \sum_{k=0}^{\infty} k^j q_{m,k} \quad (m,j = 0, ..., 3) \quad (40)$$

It should be noted that the values of $Y_{m,0}$ and $Q_{m,0}$ can also be obtained by directly solving the equations obtained by summing up for all i values eqs 27−29 and 36 for $y_{0,i}$ and $q_{0,i}$. Besides $Y_{0,0}$ given by eq 18, the overall moments $Y_{1,0}$, $Y_{2,0}$, $Q_{0,0}$, $Q_{1,0}$, and $Q_{2,0}$ are obtained by summing up for all i values equations 30−32, 33−35, 36, 37, and 38, respectively. The following equations are thus obtained:

$$\frac{dY_{1,0}}{dM_c} = \frac{\mathscr{R}_e N_A}{N}\left(\frac{N}{N_A} - Y_{0,0}\right) + 1 + C_{fm}\left(1 - \frac{Y_{1,0}}{Y_{0,0}}\right) - \mathscr{R}_d + C_{fp}\left(\frac{Q_{2,0}}{M} - \frac{Q_{1,0}}{M}\frac{Y_{1,0}}{Y_{0,0}}\right) + C_p^*\alpha\frac{Q_{1,0}}{M} + 2C_{ex1}\frac{T_2}{M}\left(1 - \frac{Y_{1,0}}{Y_{0,0}}\right) + C_{ex}\left(\frac{Q_{1,1}}{M} - \frac{Y_{1,0}}{Y_{0,0}}\frac{Q_{0,1}}{M}\right) - Y_{1,0}\frac{\mathscr{R}_e N_A}{N} \quad (41)$$

$$\frac{dY_{2,0}}{dM_c} = \frac{\mathscr{R}_e N_A}{N}\left(\frac{N}{N_A} - Y_{0,0}\right) + 1 + 2\frac{Y_{1,0}}{Y_{0,0}} + C_{fm}\left(1 - \frac{Y_{2,0}}{Y_{0,0}}\right) + C_{fp}\left(\frac{Q_{3,0}}{M} - \frac{Q_{1,0}}{M}\frac{Y_{2,0}}{Y_{0,0}}\right) + C_p^*\alpha\left[\frac{Q_{2,0}}{M} + 2\frac{Q_{1,0}}{M}\frac{Y_{1,0}}{Y_{0,0}}\right] + 2C_{ex1}\frac{T_2}{M}\left(1 - \frac{Y_{2,0}}{Y_{0,0}}\right) + C_{ex}\left(\frac{Q_{2,1}}{M} - \frac{Y_{2,0}}{Y_{0,0}}\frac{Q_{0,1}}{M}\right) - \mathscr{R}_d - Y_{2,0}\frac{\mathscr{R}_e N_A}{N} \quad (42)$$

$$\frac{dQ_{0,0}}{dM_c} = C_{fm} - C_p^*\alpha\frac{Q_{0,0}}{M} + 2C_{ex1}\frac{T_2}{M} + Y_{0,0}\frac{\mathscr{R}_e N_A}{N} \quad (43)$$

$$\frac{dQ_{1,0}}{dM_c} = C_{fm}\frac{Y_{1,0}}{Y_{0,0}} - C_{fp}\left(\frac{Q_{2,0}}{M} - \frac{Q_{1,0}}{M}\frac{Y_{1,0}}{Y_{0,0}}\right) - C_p^*\alpha\frac{Q_{1,0}}{M} + 2C_{ex1}\frac{Y_{1,0}}{Y_{0,0}}\frac{T_2}{M} + C_{ex}\left(-\frac{Q_{1,1}}{M} + \frac{Q_{0,1}}{M}\frac{Y_{1,0}}{Y_{0,0}}\right) + Y_{1,0}\frac{\mathcal{R}_e N_A}{N} \quad (44)$$

$$\frac{dQ_{2,0}}{dM_c} = C_{fm}\frac{Y_{2,0}}{Y_{0,0}} - C_{fp}\left(\frac{Q_{3,0}}{M} - \frac{Q_{1,0}}{M}\frac{Y_{2,0}}{Y_{0,0}}\right) - C_p^*\alpha\frac{Q_{2,0}}{M} + 2C_{ex1}\frac{Y_{2,0}}{Y_{0,0}}\frac{T_2}{M} + C_{ex}\left(-\frac{Q_{2,1}}{M} + \frac{Q_{0,1}}{M}\frac{Y_{2,0}}{Y_{0,0}}\right) + Y_{2,0}\frac{\mathcal{R}_e N_A}{N} \quad (45)$$

Finally, the values of the main average quantities of the polymer MWD are obtained from the values of the overall moments as follows:

$$M_n = \frac{Y_{1,0} + Q_{1,0}}{Y_{0,0} + Q_{0,0}}; \quad M_w = \frac{Y_{2,0} + Q_{2,0}}{Y_{1,0} + Q_{1,0}}; \quad P_d = \frac{M_w}{M_n} \quad (46)$$

where M_n indicates the number average degree of polymerization, M_w indicates the weight average, and P_d indicates the polydispersity ratio.

8. Nomenclature

a	desorption parameter defined in eq 2, m^2/s
C_x	ratio of the effective rate constant, K_x, to the effective rate constant of propagation, K_p
(CF_2H)	concentration of CF_2H end groups, $kmol/m_w^3$
(CF_2I)	concentration of CF_2I end groups, $kmol/m_w^3$
(CH_2OH)	concentration of CH_2OH end groups, $kmol/m_w^3$
(CH_3)	concentration of CH_3 end groups, $kmol/m_w^3$
D_w	radical diffusion coefficient in water phase, m^2/s
D_p	radical diffusion coefficient in particle, m^2/s
h_i	Henry constant of the ith monomer, $kmol/Mpa/m_w^3$
I	initiator concentration, $kmol/m_w^3$
k_{bbi}	rate constant of back biting for the ith radical, $kmol/m_p^3/s$
k_d	rate constant of radical desorption, 1/s
k_e	rate constant of radical entry, m_w^3/s/particle
$k_{ex,i}$	rate constant of degenerative transfer of radical i to transfer agent, $kmol/m_w^3/s$
k_{ex1}	rate constant of degenerative transfer of radical i to dormant chain, $kmol/m_p^3/s$
k_{fmij}	rate constant of chain transfer of radical i to monomer j, $kmol/m_p^3/s$
k_{fpij}	rate constant of chain transfer of radical i to polymer (monomer unit of type j), $kmol/m_p^3/s$
k_I	rate constant of initiator decomposition, 1/s
$k_{p,ij}$	rate constant of propagation of radical i to monomer j, $kmol/m_p^3/s$
K_{bb}	effective (composition average) rate constant of back biting, $kmol/m_p^3/s$
K_{ex}	effective (composition average) rate constant of degenerative transfer to transfer agent, $kmol/m_p^3/s$
K_{ex1}	effective (composition average) rate constant of degenerative transfer to dormant chain, $kmol/m_p^3/s$
K_{fm}	effective (composition average) rate constant of chain transfer to monomer j, $kmol/m_p^3/s$
K_{fp}	effective (composition average) rate constant of chain transfer to polymer (monomer unit of type j), $kmol/m_p^3/s$
K_p	effective (composition average) rate constant of propagation, $kmol/m_p^3/s$
K_p^*	effective (composition average) rate constant of propagation to TDB, $kmol/m_p^3/s$
(LCB)	concentration of long chain branches, $kmol/m_w^3$
m	partition coefficient of radicals between water phase and particles
M_i	concentration of monomer i in particle, $kmol/m_w^3$
M_i^g	concentration of monomer i in gas phase, $kmol/m_w^3$
M_i^T	overall concentration of monomer i in the reactor, $kmol/m_w^3$
M_c	concentration of consumed monomer mixture, $kmol/m_w^3$
N	concentration of polymer particles, $particle/m_w^3$
N_A	Avogadro's number, molecules/mol
P	pressure, MPa
$P_{n,i}$	concentration of dead chains with n monomer units and i iodine terminal units, $kmol/m_w^3$
$q_{n,i}$	moment of the dead chain distribution of order n with respect to monomer units and with i iodine terminal units, $kmol/m_w^3$
Q	feed flowrate of monomer mixture, kmol/s
$Q_{m,j}$	overall moment of the dead chain distribution of orders m and j with respect to monomer units and iodine terminal units, respectively, $kmol/m_w^3$
r	particle radius, m
R	ideal gas constant, MPa m^3/kmol K
$R_{n,i}$	concentration of active chains with n monomer units and i iodine terminal units, $kmol/m_w^3$
R_W	concentration of active chains in water phase, $kmol/m_w^3$
$\mathcal{R}_d'$	overall desorpion rate, $kmol/m_w^3$ s
$\mathcal{R}_e'$	overall entry rate, $kmol/m_w^3$ s
$\mathcal{R}_I'$	overall rate of initiator decomposition, $kmol/m_w^3$ s
$\mathcal{R}_d$	desorpion rate specific to the molar amount of consumed monomer mixture
$\mathcal{R}_e$	entry rate specific to the molar amount of consumed monomer mixture
$\mathcal{R}_I$	rate of initiator decomposition specific to the molar amount of consumed monomer mixture
(SCB)	concentration of short chain branches, $kmol/m_w^3$
T	temperature, K
T_2	concentration of iodine transfer agent, $kmol/m_w^3$
(TDB)	concentration of terminal double bonds, $kmol/m_w^3$
V_g	volume of gas phase in the reactor, m^3
V_p	volume of particle phase in the reactor, m_p^3
V_W	volume of water phase in the reactor, m_w^3
w_i	mole fraction of monomer i in the feed
y_i	mole fraction of monomer i in the gas phase
$y_{n,i}$	moment of the active chain distribution of order n with respect to monomer units and with i iodine terminal units, $kmol/m_w^3$
Y_i	mole fraction of monomer i in the copolymer

$Y_{m,j}$ overall moment of the active chain distribution of orders m and j with respect to monomer units and iodine terminal units, respectively, kmol/m_w^3

z compressibility factor of the gas mixture

Greek Letters

α average number of terminal double bonds in the terminated chain

β fraction of backbiting reactions forming CF_2H chain ends

η initiator efficiency

Φ_j probability of having an active chain with terminal unit of monomer j

ρ_c copolymer density, kg/m_p^3

References and Notes

(1) Apostolo, M.; Arcella, V.; Storti, G.; Morbidelli, M. *Macromolecules* **1999**, *32*, 989.

(2) Matyjaszewski, K. In *Controlled Radical Polymerization*; ACS Symposium Series No. 685; Matyjaszewski, K., Ed.; ACS: Washington, DC, 1998; p 2.

(3) Szwarc, M. *Carbanions, Living polymers, and Electron-Transfer Processes*; Wiley: New York, 1968.

(4) (a) Matyjaszewski, K.; Gaynor, S. C.; Wang, J. S. *Macromolecules* **1995**, *28*, 2093. (b) Gaynor, S. C.; Wang, J. S.; Matyjaszewski, K. *Macromolecules* **1995**, *28*, 8051. (c) Pattern, T. E.; Matyjaszewski, K. *Adv. Mater.* **1998**, *10*, 901. (d) Goto, A.; Ohno, K.; Fukuda, T. *Macromolecules* **1998**, *31*, 2809.

(5) Butté, A.; Storti, G.; Morbidelli, M. *Macromolecules* **2001**, *34*, 5885.

(6) Oka, M.; Tatemoto, M. *Contemporary Topics in Polymer Science*; Plenum Press: New York, 1984; Vol. 4, p 763.

(7) Apostolo, M.; Albano, M.; Storti, G.; Morbidelli, M. *Macromol. Symp.* **2000**, *150*, 65.

(8) (a) Giannetti, E.; Visca, M. U.S. Patent No. 4,486,006, 1988. (b) Giannetti, E.; Chittofrati, A.; Sanguineti, A. *Chim. Ind., Spec. Fluoro* **1997**, *79*, 22.

(9) Logothetis, A. *Prog. Polym. Sci.* **1989**, *14*, 251.

(10) (a) Mueller, A. H. E.; Zhuang, R. G.; Yan, D. Y.; Litvinenko, G. *Macromolecules* **1995**, *28*, 4326. (b) Mueller, A. H. E.; Yan, D. Y.; Litvinenko, G.; Zhuang, R. G.; Dong, H. *Macromolecules* **1995**, *28*, 7335. (c) Litvinenko, G.; Mueller, A. H. E. *Macromolecules* **1997**, *30*, 1253. (d) Lansalot, M.; Farcet, C.; Charleux, B.; Vairon, J. P.; Pirri, R. *Macromolecules* **1999**, *32*, 7354. (e) Butté, A.; Storti, G.; Morbidelli, M. *Macromolecules* **2000**, *33*, 3485.

(11) Apostolo, M.; Morbidelli, M. *Chim. Ind., Spec. Fluoro* **1997**, *79*, 361.

(12) (a) Drott, E. E.; Mendelson, R. A. J. *Polym. Sci.: Part A2* **1970**, *8*, 1361. (b) Ram, A.; Miltz, J. J. *Appl. Polym. Sci.* **1971**, *15*, 2639. (c) Hamielec, A. E. *Pure Appl. Chem.* **1982**, *54*, 293.

(13) Maccone, P.; Apostolo, M.; Ajroldi, G. *Macromolecules* **2000**, *33*, 1656.

(14) Gianotti, G.; Leolini, C.; Borghi, D. *Chim. Ind.* **1991**, *73*, 463.

(15) Gilbert, R. G. *Emulsion Polymerization: A Mechanistic Approach*; Academic Press: San Diego, CA, 1995; Chapter 3.

(16) Asua, J. M.; Sudol, E. D.; El-Aasser, M. S. J. *Polym. Sci.: Part A: Polym. Chem.* **1989**, *27*, 3903.

(17) Howe-Grant, M., Ed.; *Fluorine Chemistry: A Comprehensive treatment*; Wiley; New York, 1995; p 275.

(18) Zhu, S.; Hamielec, A. E. J. *Polym. Sci.: Part B: Polym. Phys.* **1994**, *32*, 929.

(19) (a) Xie, T.; Hamielec, A. E. *Makromol. Chem., Macromol. Symp.* **1993**, *2*, 455. (b) Storti, G.; Carrá, S.; Morbidelli, M.; Vita, G. J. *Appl. Polym. Sci.* **1989**, *37*, 2443.

(20) Martin, J. J. *Ind. Eng. Chem. Fundam.* **1979**, *18*, 81.

(21) Dotson, N. A.; Galvan, R.; Laurence, L. R.; Tirrell, M. In *Polymerization Process Modeling*; VCH Publishers Inc.: New York, 1996; p 45.

(22) Hulburt, H. M.; Katz, S. *Chem. Eng. Sci.* **1964**, *19*, 555.

(23) Baltsas, A.; Achilias, D. S.; Kiparissides, C. *Macromol. Theory Simul.* **1996**, *5*, 477.

(24) Arcella, V.; Brinati, G.; Apostolo, M. *Chim. Ind.* **1997**, *79*, 345.

(25) Kolthoff, I. M.; Miller, I. K. *J. Am. Chem. Soc.* **1951**, *73*, 3055.

(26) Apostolo, A. Ausimont Internal Report No. 1/97; Ausimont R&D: Bollate, Italy, 1997.

MA0119575